Coating and Structural Locking of Dipolar Chains of Cobalt Nanoparticles

Zhihan Zhou, Guojun Liu,* and Dehui Han

Department of Chemistry, Queen's University, 90 Bader Lane, Kingston, Ontario, K7L 3N6

ABSTRACT Above a critical size, Co nanoparticles aggregate because of magnetic dipole−dipole interaction into chains. Reported in this paper is the coating of such chains by an AB diblock copolymer in a block-selective solvent for the A block. Also reported is the cross-linking of the deposited or anchored B block of the diblock copolymer to lock in the coating and thus the dipolar chain structure. The Co nanoparticles used were prepared from the high-temperature decomposition of $Co_2(CO)_8$ using poly(2-cinnamoyloxyethyl methacrylate)-*block*-poly(acrylic acid) or PCEMA-*b*-PAA as surfactant. To coat the dipolar chains, the particles and diblock copolymer poly(*tert*-butyl acrylate)-*block*-poly(2-cinnamoyloxyethyl methacrylate), PtBA-*b*-PCEMA, were dispersed in a good solvent for PCEMA and PtBA. Methanol, a precipitant for PCEMA and a good solvent for PtBA, was then added. This induced the collapsing of the PCEMA blocks and the deposition of the PCEMA block of PtBA-*b*-PCEMA onto the surface of PCEMA-*b*-PAA-coated Co nanoparticle chains. The dipolar chains remained colloidally stable in solution for steric stabilization provided by PtBA. The coating was cured by photocrosslinking the PCEMA layer. Such "permanent" and solvent-dispersible Co dipolar chains are novel and may have interesting applications.

KEYWORDS: Co nanoparticles · magnetic nanoparticles · magnetic dipolar chains · polymer brush · block copolymers · cross-linking

Above a critical size, Co nanoparticles may overcome repulsion provided by the coating surfactant molecules and aggregate because of magnetic dipole−dipole interaction into chain-like structures.[1,2] Such structures include linear chains, loops, networks, and 3-d suprastrctures as have been predicted theoretically[3−5] and verified experimentally.[1,2,6,7] While such structures can be beautiful, they are normally not very stable. Multiple rinsing of Co nanoparticles by a good solvent for the surfactant normally leads to surfactant removal and the precipitation of the Co nanoparticles.[8] The locking of such aggregated structures *via* the cross-linking of the coating surfactant molecules may yield interesting materials with novel applications. For example, one can imagine the locking of a 3-d network structure to yield a porous film.[9] Such a polymer-coated Co dipolar chain network may contract or expand in the presence or absence of a magnetic field and may be useful in controlled release applications. While many obstacles need to be overcome before the preparation of such a material, we report in this paper our first step toward such a goal. This involves the coating of linear dipolar chains of Co nanoparticles by a diblock copolymer and the cross-linking of the anchoring layer of the coating copolymer to yield "permanent" polymer-coated Co nanoparticle chains.

More specifically, the Co nanoparticles used were prepared from the high temperature decomposition of $Co_2(CO)_8$ utilizing a diblock copolymer poly(2-cinnamoyloxyethyl methacryate)-*block*-poly(acrylic acid), PCEMA-*b*-PAA or polymer I, as surfactant. The polymer had 30 CEMA units and 4 AA units. The resultant particles were coated by PCEMA-*b*-PAA with PAA anchoring on the Co surface and the PCEMA block stretching into the solvent phase (A, Scheme 1). The Co nanoparticles aggregated into linear chains spaced by PCEMA-*b*-PAA for the magnetic dipole−dipole interaction (A→B, Scheme 1). To build a fully protecting layer for the dipolar chains, we mixed them in a solvent with another diblock copolymer poly(*tert*-butyl acrylate)-*block*-poly(2-cinnamoyloxyethyl methacrylate), PtBA-*b*-PCEMA or polymer II, consisting of 290 tBA units and 100 CEMA units. To the solution was then added methanol, a block selective solvent for PtBA. Above a sufficiently high methanol content, the PCEMA blocks of Polymers I and II collapsed from the solvent phase and the coated dipolar chains were rendered colloidally stable by the PtBA chains (B→C). Photolysis of such a mixture with UV light led to the cross-linking of the collapsed PCEMA layer (C→D) and the structural locking of the dipolar chains.

*Address correspondence to guojun.liu@chem.queensu.ca.

Received for review August 26, 2008 and accepted December 05, 2008.

Published online December 15, 2008.
10.1021/nn8005366 CCC: $40.75

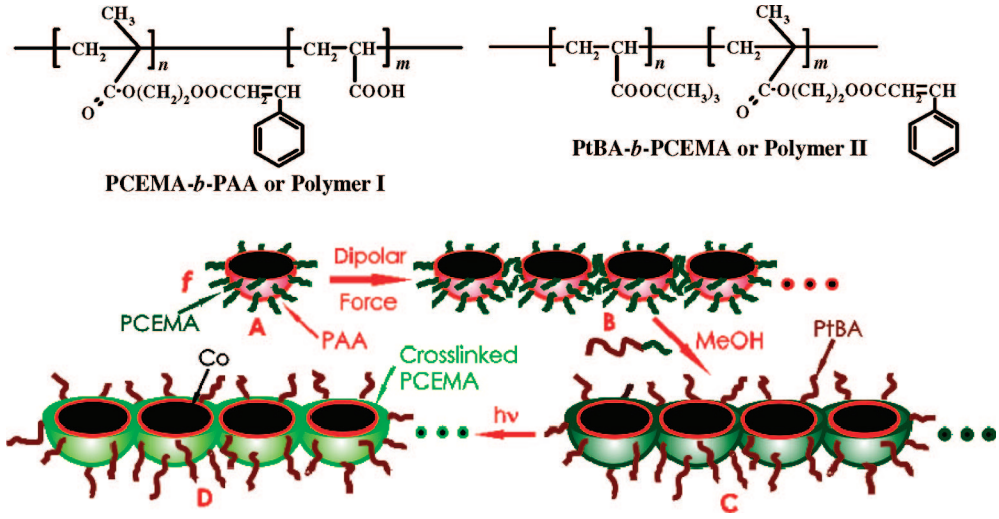

Scheme 1. Cross-sectional schematic for formation (A→B), coating (B→C), and structural locking (C→D) of a Co dipolar chain.

While we are unaware of reports on the preparation of solvent-dispersible cross-linked Co dipolar chains, Co nanoparticle chains have been assembled at an oil/water interface and have been "fossilized" or frozen onto the oil phase surface by the quick photocrosslinking or gelling of the oil.[10,11] Also dipolar chains of polymer-coated Co nanoparticles have been pyrolyzed to yield carbon-coated Co nanofibers.[12] Going beyond Co, there have been reports on polymer/Ni or polymer/γ-Fe_2O_3 hybrid nanofibers[13−15] obtained from the production of Ni or γ-Fe_2O_3 in the cores of preformed triblock copolymer nanotubes. There have been also reports on the preparation of superparamagnetic chains from the interlinking of polymer/magnetite composite microspheres with sizes typically larger than 500 nm.[16−20] The movement of such chains in a rotating magnetic field has been shown to facilitate reagent mixing in microfluidic channels.[21] The passing of a DNA solution through a standing array of such chains has helped the separation of DNA of different sizes.[22]

RESULTS AND DISCUSSION

Co Nanoparticle Sample 1. There have been many reports on the preparation of Co nanocrystals with different geometries.[18] Co nanoparticles have been prepared typically from two methods at high temperatures. Method 1 involves the high temperature decomposition of a Co(0) precursor such as $Co_2(CO)_8$ in the presence of a surfactant (*e.g.*, oleic acid) and a cosurfactant (*e.g.*, TOPO).[23,24] The surfactants were used to regulate the growth and to render colloidal stability to the final Co nanoparticles. TOPO, binding reversibly to Co, was used mainly to narrow the particle size distribution. Method 2 involves the reduction of Co^{2+} in the presence of a surfactant and cosurfactant.[25,26] Aside from using small-molecule surfactants, random copolymers,[27,28] block copolymers,[8,29] and end-functionalized copolymers[6] have also been used as surfactant.

We prepared Co nanoparticle sample 1 from the high temperature decomposition of $Co_2(CO)_8$ in dichlorobenzene using polymer I and TOPO as the surfactant and cosurfactant. We used a double injection protocol for the precursor $Co_2(CO)_8$ because it helped yield particles with narrower size distributions as discovered and justified by Peng *et al.*[30] After each preparation, the particles were purified by magnetic decantation, which involved the capturing of the particles on the wall of a vial next to a magnet and the removal of dichlorobenzene. The particles were redispersed in chloroform. Shown in Figures 1a and 1b are TEM images for such a sample aspirated from chloroform on carbon-coated copper grids.

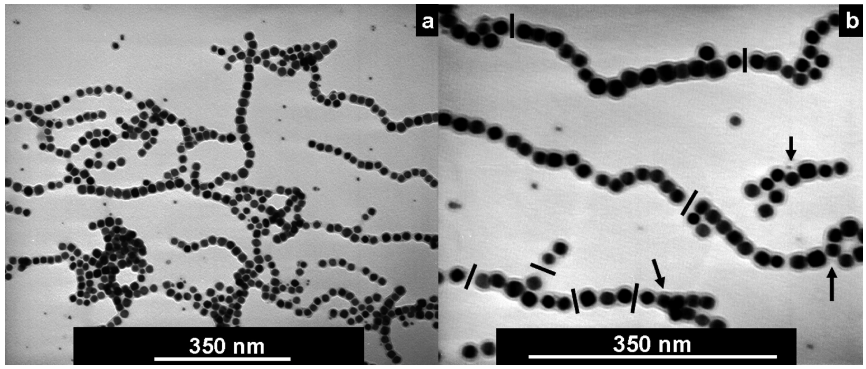

Figure 1. TEM images of Co nanoparticle sample 1 aspirated on carbon-coated copper grid at low (a) and high (b) magnifications. Only the specimen for Figure 1b was stained by OsO_4.

These images reveal the following features about the particles. First, the particles had a core−shell structure as seen in Figure 1b. The core must have consisted of the more strongly electron-diffracting Co nanocrystal, and the shell must have consisted of PCEMA-*b*-PAA. The shell thickness was

measured along the line that coincided with the radial direction of each constituent Co nanoparticle and that of the dipolar chain. The average of over more than 100 particles was 5.5 ± 0.7 nm for this sample. Second, the particles had a relatively narrow size distribution in agreement with results reported for another polymer−ligand-based synthesis.[6] Averaging over more than 100 Co nanocrystals, we obtained an average Co core diameter of 19.4 ± 2.1 nm for this sample. Third, most of the particles were in an aggregated form. Rather than aggregation into compact 3-d clusters, which were products expected if the nondirectional or isotropic van der Waals attraction operated between the different particles, the particles aligned into linear chains and branched chains (marked by arrows). Fourth, the average spacing or the closest distance between two neighboring Co particles in the dipolar chains was 3.6 ± 1.0 nm. To obtain this average, we excluded these pairs of particles marked by dark lines Figure 1b, because they had a separation distance larger than 6 nm and appeared to belong to different dipolar chains or to be in a transition to dissociate or associate.

Since the binding energy should be much higher for the AA units than for the CEMA units,[31] polymer I should bind to the Co nanoparticle surfaces *via* the PAA block as depicted in Scheme 1. The diblock consisted of a total of 34 units for CEMA and AA. The length of such a fully stretched chain is 8.6 nm. Assuming a characteristics ratio C_∞ of 6.0, a typical value for atactic poly(methyl methacrylate),[32] the root-mean-square end-to-end distance of such a chain in the unperturbed state was estimated to be 3.1 nm. The fact that the layer thickness was between 3.1 and 8.6 at 5.5 nm was reasonable.

While linear and branched chains are all theoretically predicted structures formed from the self-assembly of dipolar particles,[9] we should be cautious in concluding about the true existence of the branched chains in the solution phase. They could have formed during chloroform evaporation or TEM specimen preparation. The linear chains must have existed already in the solution phase because they were far more ubiquitous than the branched structures. Their existence in solution has been demonstrated by various groups using techniques such as cryo-TEM[1] as well as structural locking of Co dipolar chains and then the confirmation of the chain structures by microscopy.[10] Their existence in solution in our case will be unambiguously proven by our ability to coat and lock in such structures in solution.

The average particle spacing of 3.6 nm for both batches of Co nanoparticles in dipolar chains was much smaller than 2 × 5.5 nm, with 5.5 nm being the PCEMA-*b*-PAA shell thickness. This suggests the extensive compression of the surface PCEMA chains between different particles as depicted in B of Scheme 1. Zhulina *et al.*[33] argued that two identical approaching brush layers

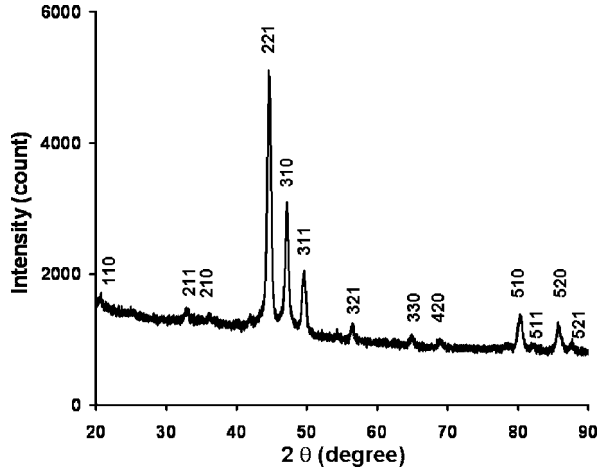

Figure 2. X-ray diffraction data for polymer-I-coated Co nanoparticles.

should each get compressed rather than undergo intermixing if the spacing between the substrates is larger than the unperturbed dimension of the polymer coils in solvent. For PCEMA with 30 repeat units, its radius of gyration should be around 1.2 nm. On the basis of these, we have thus depicted in B of Scheme 1 compressed rather than mixed PCEMA chains between two neighboring Co nanoparticles in a dipolar chain. This will be proven correct later by our experimental evidence.

The small interparticle distance in a chain suggests a strong dipolar attractive force. Quantitatively, the dipolar coupling constant λ defined as the ratio between the dipolar interaction energy and the thermal energy k_BT is[10,34]

$$\lambda = \frac{\mu^2}{4\pi\mu_r\mu_0\sigma^3 k_B T} \quad (1)$$

where μ_0, $4\pi \times 10^{-7}$ NA^{-2}, is the magnetic permeability of the vacuum; μ_r is the relative permeability for the diamagnetic chloroform or dichlorobenzene and should be close to 1;[35] σ is the overall diameter of a polymer-I-coated Co nanoparticle and was assumed to be 30.4 nm; and μ is the magnetic dipole moment of a Co particle. For a Co particle with a radius *r*, μ is given by

$$\mu = \frac{4\pi r^3 \mu_0 M_s}{3} \quad (2)$$

where M_s, the saturation magnetization of bulk Co, is 1.4×10^6 Am^{-1}.[36] Inserting eq 2 and the relevant information into eq 1, we estimated a λ value of 24.6 for Co particles with a diameter of 19.4 nm, thus confirming the strong dipole−dipole interaction.

Figure 2 shows X-ray diffraction data for the Co nanoparticles. A comparison with literature data suggests that the particles were ε-Co nanocrystals.[26,37,38] Using the data of peak 221 and peak 310 and the Scherrer equation we obtained the nanocrystal diameters of

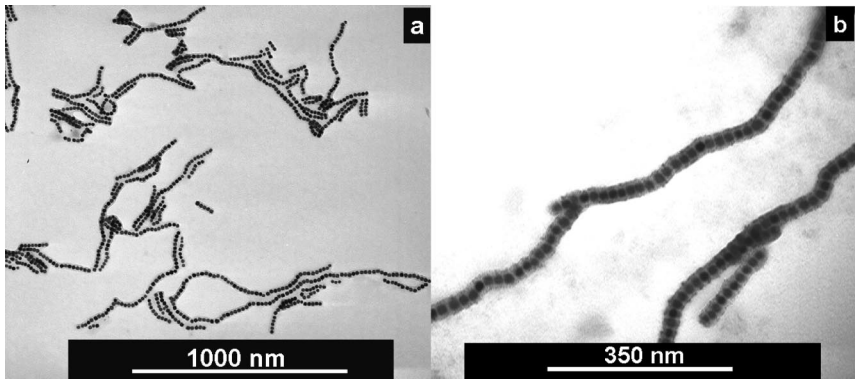

Figure 3. Low (a) and high (b) magnification TEM images of polymer-II-coated and cross-linked Co dipolar chains aspirated from $CHCl_3$ on carbon-coated copper grids.

18.4 and 19.3 nm, which are in agreement with the TEM diameter of 19.4 ± 2.1 nm for the Co nanocrystals.

We dissolved the Co cores of the nanoparticles by HCl and then titrated the Co^{2+} amount complexometrically following procedures detailed in the Supporting Information. This yielded a Co weight fraction of 70% in the nanoparticles. Using the densities of 8.9 and 1.25 g/cm^3 for Co[39] and the diblock copolymer[40] and a diameter of 19.4 nm for the Co nanoparticles, we calculated a shell thickness of 5.8 nm, which agreed with 5.5 ± 0.7 nm from TEM analysis.

We obtained from gravimetric analysis that the utilization rate for the Co element in the precursor $Co_2(CO)_8$ was 82% and that for PCEMA-*b*-PAA was lower at 67%. This lower than 100% utilization rate for Co was probably for operational sample loss and for the removal of some smaller Co nanoparticles during the magnetic decantation step.

To know the extent to which the PCEMA block had undergone thermal cross-linking during Co nanoparticle preparation, a control experiment was performed. In this experiment, PCEMA-*b*-PAA was subjected to the same heat treatment that it would have received in a normal Co nanoparticle preparation protocol except that $Co_2(CO)_8$ was not used. The polymer was then analyzed spectrophotometrically for PCEMA absorbance analysis at 278 nm. This yielded a CEMA double bond conversion of 14%.[41]

Coating and Structural Locking of the Co Dipolar Chains. To coat the dipolar chains, we mixed the Co nanoparticles with polymer II and then added methanol slowly. Being insoluble in methanol, the PCEMA block of polymer I should precipitate from the solvent phase above a critical methanol content. Being longer, the PCEMA block of polymer II should precipitate out before the PCEMA block of polymer I. Obviously these two blocks should be compatible. The PCEMA block of polymer II spread on the surface of the dipolar chains, and the PtBA chains stretched into the solvent phase. Thus, polymer II formed a brush layer[42−45] on the dipolar chain surface as depicted in Scheme 1. The dipolar chains remained dispersed in $CHCl_3$/MeOH because of steric stabilization provided by the soluble PtBA block of polymer II.[46]

Once the dipolar chains were coated by polymer II, we used a standard protocol as described in the Experimental Section for the photolysis of the resultant samples to produce "permanent" polymer/Co chains. Such samples, referred from now on as Co sample 2, normally had a PCEMA double bond conversion of ~43% from photolysis.

We experimented with different Co sample 1 to polymer II weight ratios and found out that a mass ratio of ~1/1 worked the best. The use of too much polymer II yielded samples containing many cross-linked micellar particles of polymer II as the background in TEM images. The use of too little polymer II led to samples that could not redisperse in solvents after they were vacuum-dried into solid. However, the use of excess polymer II did not present any technical challenges because the cross-linked micelles were readily separated from the dipolar chains by magnetic decantation.

Figure 3 shows TEM images of Co sample 2. The sample was coated and cross-linked using the optimized protocol. The dipolar chain structure of Figure 1 was clearly retained here. The TEM image of Figure 3b shows the thickness of the stainable PCEMA layer had increased from 5.5 ± 0.7 nm to 9.2 ± 1.5 nm, supporting the deposition of polymer II on the original dipolar chains.

We have determined by complexometric titration a Co weight fraction of 46% for such a sample. Assuming that the weight ratio between Co and polymer I was the same in Co samples 1 and 2, we calculated weight fractions of 34% for polymer II and 20% for polymer I in Co sample 2. Using the weight fraction of 41% for PCEMA in polymer II, we estimated that the PCEMA layer thickness in Co sample 2 with a core diameter of 19.4 nm should be at 8.2 nm. This is somewhat smaller than the TEM value of 9.2 ± 1.5 nm but is reasonable considering that the PCEMA layer of the TEM sample might be trapped in a partially swollen state after aspiration from $CHCl_3$.

Properties of the Cross-Linked Dipolar Chains. Aside from structural integrity retention as confirmed by TEM, the cross-linked Co dipolar chains retained the magnetic properties of their precursors. Figure 4 shows the magnetization curves for powders of Co samples 1 and 2 obtained at 300 K. For Co sample 1, the saturation magnetization M_S, remanence magnetization M_R, and coercivity H_C were 120 emu/g, 34 emu/g, and 0.79 kOe, respectively. These values changed to 74 emu/g, 19.0 emu/g, and 0.85 kOe for sample 2. Taking the Co weight fractions of 70% and 46% for samples 1 and 2 into consideration, the M_S and M_R values were 171 and

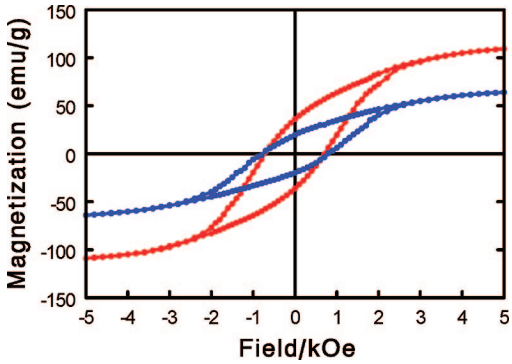

Figure 4. Magnetization curves for polymer-I-coated (rred) and polymer-II-coated and PCEMA-cross-linked (blue) Co nanoparticle powders.

49 emu per g of Co for sample 1 and 161 and 41 emu per g of Co for sample 2. The two sets of M_S, M_R, and H_C values evidently agree reasonably well with each other.

The nonzero M_R and H_C values suggest that the Co nanoparticles at a TEM diameter of 19.4 ± 2.1 nm were ferromagnetic at 300 K, a conclusion in accord with observations made by others before.[6] The M_S values of 171 and 161 emu/g of Co for samples 1 and 2 are close to the M_S value of 161 emu/g reported for bulk Co.[39] This suggests the high purity of the Co crystals. A M_S value higher than 161 emu/g of Co was obtained for sample 1 most probably for an underestimated Co content for this sample. For this sample, polymer I was not covalently attached to Co. The amount of polymer I remaining in a smaple depended on how it was rinsed by solvents. The sample used for Co content analysis was not rinsed by solvents after its precipitation from DBC/diethyl ether. On the other hand, the sample used for magnetic property measurement was rinsed twice by hexane and probably contained less polymer I and higher than 70% Co.

To know what happened to the dipolar chains in a magnetic field on the microscopic scale, we dispensed one drop of a cross-linked Co dipolar chain solution in CH_2Cl_2 on a carbon-coated TEM grid placed next to a 0.47-T magnet. After evaporation of the solvent CH_2Cl_2, we obtained TEM images with one shown in Figure 5.

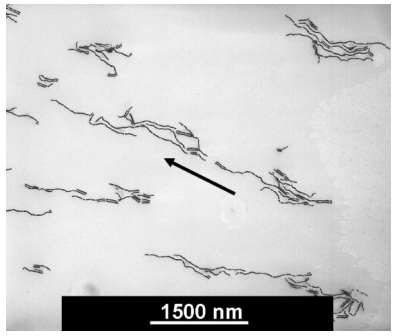

Figure 5. TEM image of polymer-II-coated and cross-linked Co dipolar chains left on a carbon-coated copper grid after solvent evaporation from one drop of the chain solution in CH_2Cl_2 in a magnetic field. The arrow denotes the magnetic field direction.

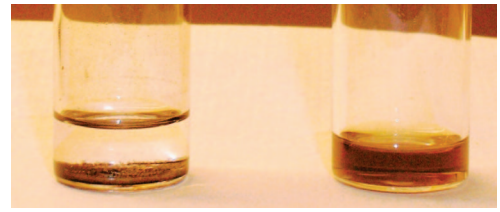

Figure 6. Photograph comparing dispersions of polymer-II-coated Co nanoparticles subjected to no UV irradiation (left) and UV irradiation (right) after rinsing by $CHCl_3$ thrice.

Some of the dipolar chains clustered in a magnetic field. Also, they had a tendency to align along the magnetic field direction. These behaviors are the same as those that we observed for triblock copolymer/γ-Fe_2O_3 hybrid nanofibers.[14]

The anticipated advantage of the cross-linked Co dipolar chains was their stability against repeated solvent rinsing. To show this, we rinsed by magnetic decantation Co dipolar chains that were coated with polymer II before and after PCEMA cross-linking. Figure 6 compares the dispersion states after $CHCl_3$ rinsing three times of two polymer-II-coated samples that were irradiated and not irradiated by UV light. Evidently, the sample that was not irradiated totally lost its dispersibility after $CHCl_3$ rinsing. We rinsed the cross-linked sample only up to 10 times and noticed no change in colloidal dispersibility of this sample. Our suspicion was that the sample would retain its colloidal stability regardless of the rinsing times. Also the cross-linked sample could be dispersed in a wide range of good solvents for PtBA and they included methanol, toluene, and tetrahydrofuran.

Solvent-dispersible Porous Nanofibers. Co could be dissolved by HCl. After Co dissolution, the polymer coating remained dispersed in the $CHCl_3$ phase. After sample aspiration on a carbon-coated TEM grid and sample staining by RuO_4, the residual polymer was analyzed by TEM with one image shown in Figure 7a.

The Figure shows that the fibers contained internal cavities once occupied by Co nanoparticles before their dissolution. Thus, such polymer/Co dipolar chains served as precursors for the preparation of solvent-dispersible porous polymer nanofibers, an architecture that should be novel.

Cross-linking of Polymer-I-Coated Co Nanoparticles. We have tried to lock in the dipolar chain structure at stage B of Scheme 1 or dipolar chains coated by polymer I. The photocrosslinking of PCEMA at this stage under conditions similar to those used for the polymer-II-coated dipolar chains did help stabilize the dipolar chains against $CHCl_3$ rinsing. The photolyzed polymer-I-coated dipolar chains, however, failed to redisperse in organic solvents such as THF and chloroform after they had been vacuum-dried. This was similar to the behavior of shell-cross-linked diblock copolymer spherical micelles that we studied before.[47] This happened probably because such particles lacked a proper steric stabilization layer,

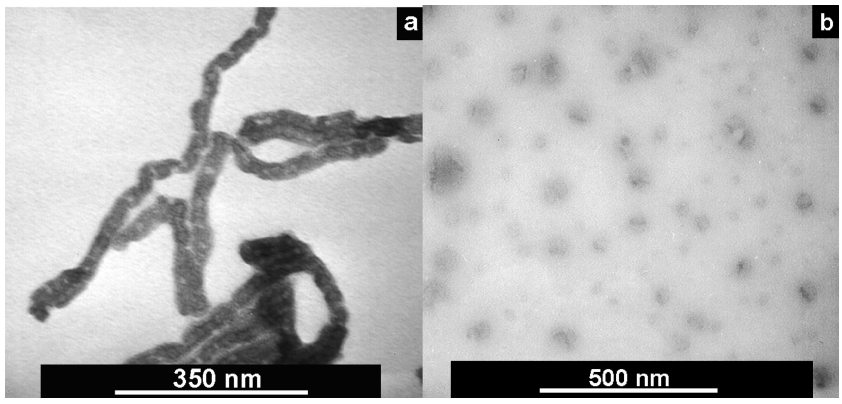

Figure 7. TEM images of polymer residuals after Co dissolution and aspiration from $CHCl_3$. Image a is for a polymer-II-coated and PCEMA-cross-linked sample and image b is for a polymer-I-coated and PCEMA-cross-linked sample.

such as the PtBA layer in Co sample 2, to provide the dispersion power for them.

Shown in Figure 7b is a TEM image of the organic residual after Co was dissolved by HCl from a polymer-I-coated and PCEMA-cross-linked dipolar chain sample. Unidentified pieces of various sizes are seen. While a detailed account of the species seen in 7b is beyond the scope of this paper, what is clear here is the absence of the fiber-like structures as seen in Figure 7a. This suggests little reaction between polymer I chains attached to different Co particle surfaces and confirms our prior assertion that PCEMA chains of neighboring particles did not undergo much intermixing.

CONCLUSIONS

$PCEMA_{30}$-*b*-PAA_4 and $PtBA_{290}$-*b*-$PCEMA_{100}$ have been synthesized and characterized. Using $PCEMA_{30}$-*b*-PAA_4 as a surfactant, uniform Co nanoparticles coated by $PCMEA_{30}$-*b*-PAA_4 have been prepared from the high temperature decomposition of $Co_2(CO)_8$. At a Co diameter of 19.4 ± 2.1 nm, the Co weight fraction in such particles was determined by complexiometric titration of Co^{2+} after Co dissolution by HCl to be 70%. The thickness of the $PCMEA_{30}$-*b*-PAA_4 layer was determined by TEM to be 5.5 ± 0.7 nm. The Co nanoparticles aggregated, due to magnetic dipole−dipole interaction, into dipolar chains. Adding methanol into a mixture containing an approximately equal weight of the dipolar chains and $PtBA_{290}$-*b*-$PCEMA_{100}$ in chloroform to a methanol volume fraction of 80% led to the deposition of $PtBA_{290}$-*b*-$PCEMA_{100}$ onto the dipolar chain surfaces. The dipolar chains remained stable colloidally in solution for steric stabilization provided by the PtBA chains. The PCEMA layer was cured by photolysis. Such "permanent" and solvent-dispersible dipolar chains were stable against solvent rinsing, retained the magnetic properties of their precursors, were novel, and may have interesting applications.

EXPERIMENTAL SECTION

Materials. Trioctylphosphine oxide (TOPO, 99%), cinnamoyl chloride (98%), trifluoroacetic acid (TFA, 99%), xylanol orange indicator, ethylenediaminetetraacetic acid disodium salt dehydrate (EDTA, ACS grade), sodium acetate (anhydrous), sodium hydroxide (97%), calcium chloride (Technical grade), and calcium hydride (95%) were purchased from Sigma-Aldrich and were used as received. Solvent 1,2-dichlorobenzene (DCB, Aldrich, anhydrous, 99%) was washed with concentrated H_2SO_4 once and deionized water thrice. It was then predried by $CaCl_2$ for 24 h and further dried by refluxing with CaH_2 for another 24 h at 80 °C. It was distilled under vacuum just before use. Cobalt carbonyl [$Co_2(CO)_8$, Fluka, 90−95%] was added in a N_2-filled glovebox into DCB to yield a solution at 100 mg/mL before use. Chloroform (ACS grade), methanol (ACS grade), methylene chloride (ACS grade), diethyl ether (ACS grade), hydrochloric acid (36.5%−38% or 12 M), tetrahydrofuran (THF, ACS grade), and sulfuric acid (96%−98%) were purchased from Fisher Scientific Ltd. and were used as received. Pyridine was purchased from Fisher Scientific Ltd. and was dried by passing it through two columns of alumina.

Diblock Copolymers. Since the typical protocol for the preparation[48,49] and characterization[50,51] of these block copolymers has been reported by our group before, they are not repeated here. Polymer I was characterized in the PCEMA-*b*-PtBA form for the similar solubility for PCEMA and PtBA. The repeat unit number ratios *n*/*m* for both polymers were obtained from comparing the ^{1}H NMR peak intensities of the different blocks. The specific refractive index increment dn_r/dc and the light scattering (LS) molecular weight M_w of the copolymers were determined in butanone. The polydispersity indices M_w/M_n of the samples were measured by size-exclusion chromatography (SEC) in THF based on polystyrene standards. By combining the *n*/*m* ratios and light scattering M_w values, the weight-average repeat unit numbers n_w and m_w for each diblock copolymer were calculated (Table 1). Polymer I consisted of 30 CEMA and 3.6 or 4 AA units. Polymer II consisted of 290 tBA and 100 CEMA units.

TABLE 1. Molecular Properties of Polymers I and II

polymer	SEC M_w/M_n	dn_r/dc (mL/g)	LS $10^{-4} \times M_w$ (g/mol)	NMR *n*/*m*	n_w	m_w
I [a]	1.04	0.21	0.83	8.0/1.0	30	4
II	1.08	0.117	6.4	2.9/1.0	290	100

[a] Characterized in the PCEMA-*b*-PtBA form.

Synthesis of Co Nanoparticle Sample 1. Three batches of Co nanoparticle sample 1 were prepared under identical conditions and were found by microscopy analyses to possess essentially identical sizes and shell thickness. The preparation of one batch of nanoparticles involved discharging polymer I, 36.8 mg, and TOPO, 4.5 mg, into a 50-mL two-neck round-bottom flask. The flask and the connected condenser were sealed with rubber septa. The system was evacuated and back-filled by N_2. This process was repeated five times before 3.0 mL of freshly distilled DCB was injected into the flask. The solution was heated to 180 °C within 20 min in an oil bath. Under vigorous stirring, 1.00 mL of $Co_2(CO)_8$ solution in DCB at 100 mg/mL was rapidly injected into the flask. Two minutes later, another 1.0 mL of $Co_2(CO)_8$ solution was rapidly injected into the flask. The mixture was stirred at 180 °C for 10 min. After this, the heater was turned off, and the solution was allowed to cool to room temperature over ~30 min. The solution was transferred into a glass vial for storage.

Yield Analysis. Yield for one batch of Co nanoparticle sample 1 was determined gravimetrically. This involved first adding into a preweighed vial 0.714 g (~0.55 mL) of the synthesized cobalt nanoparticle dispersion in DCB. Roughly 0.6 mL of diethyl ether was then added to precipitate the particles. The precipitate was held down to the bottom of the vial by a 0.47-T magnet, and the supernatant was removed. Our separate experiment demonstrated that polymer I at this DCB/diethyl ether volume ratio remained dispersed in the solvent phase. The precipitate was subsequently dried under vacuum for 24 h before being weighed. The yield, defined as the ratio of weight of polymer-I-coated Co nanoparticles to that of polymer I and Co fed into the system, was 77%.

Co Nanoparticle Sample 2. Into a glass vial 0.645 g (~0.50 mL) of a Co sample 1 dispersion at 16 mg/mL in DCB was charged. The cobalt particles were captured by a magnet at 0.47 T, and the DCB was removed. The captured polymer-I-coated Co nanoparticles were redispersed in 5.00 mL of $CHCl_3$, which is a good solvent for both PCEMA and PtBA. Polymer II, 9.0 mg, was added into the dispersion. The mixture was vortexed for 3 min before it was transferred into a 250-mL two-neck round-bottom flask. The mixture was stirred mechanically at 100 rpm for 5 min before 20 mL of methanol, a precipitant for PCEMA, was added over 5 min. This was followed by the immediate transfer of the resultant mixture into a 30-mL cross-linking cell and photolysis of the mixture for 24 h to cross-link PCEMA. The light beam was from a 500-W mercury lamp in an Oriel 6140 lamp housing powered by an Oirel 6128 power supply. Short-wavelength light was removed by passing it through a 270-nm cutoff filter.

The cross-linked cobalt nanoparticle chains were stable against repeated solvent rinsing. Placing such a dispersion against a magnet with a field strength of 0.47 T for 10 min allowed essentially the full capture of the particles. This was followed by the decantation of $CHCl_3$. The particles or chains were redispersed in $CHCl_3$ and were subjected to the magnetic decantation rinsing treatment thrice before physical analysis and characterization. The final yield of the polymer-II-coated and PCEMA-cross-linked dipolar chains was 4.9 mg.

Magnetic Property Measurements. Magnetization curves of Co nanoparticle samples 1 and 2 were measured at 300 K on a Quantum Design SQUID magnetometer. The amount used for the first powder sample was 5.81 mg and that for the second sample was 4.12 mg. To obtain sample 1, a cobalt particle dispersion (1.5 mL in DCB at 16 mg/mL) was placed next to a 0.47-T magnet for 2 h to capture the Co nanopartricles. The solvent was removed by a pipet before 5.0 mL of hexane was added. The solid was vortexed with hexane and the solid was captured once again by the magnet. The rinsing step was repeated another time to fully remove DCB. The cobalt particles were then dried under vacuum for 2 d to yield the solid. Sample 2 solid was obtained by placing a sample 2 solution in $CHCl_3$ next to the magnet to capture the solid. The solid was dried under vacuum.

TEM Analyses. Transmission electron microscopy (TEM) images were obtained using a Hitachi H-7000 instrument operated at an acceleration voltage of 75 kV. For viewing the Co cores, the samples were aspirated on carbon-coated copper grids and were analyzed directly without further staining. To view the polymer layer, aspirated samples were stained by OsO_4 or RuO_4 vapor for 30 min before analyses.

X-Ray Diffraction Analysis. Fifty milligrams of Co sample 1 were mounted as a thin layer on a Si disk. The sample was scanned with a Philips X'Pert Pro MPD diffractometer fitted with an X'Celerator high speed strip detector. Co Kα radiation (Fe filtered) was used. Count time was 40 s at 0.02° 2θ increments. The sample was rotated at 2 s/revolution. The final scan pattern was converted to that obtained using Cu radiation in the 2θ range of 17°−96°. The average size of the Co nanocrystals was calculated using the Scherrer equation:[52]

$$d_X = \frac{K\lambda}{\delta_{2\theta} \cos \theta} \qquad (3)$$

where the wavelength λ of X-ray used was λ = 0.15418 nm; $\delta_{2\theta}$ was the width of a peak at half-maximum; θ was the diffraction angle, and *K* was 1.107 for spherical particles.

Acknowledgment. NSERC of Canada is thanked for sponsoring this research. GL thanks the Canada Research Chairs program for a research chair position in Materials Science. Drs. Paul Dube and Graeme Luke of McMaster's University are gratefully acknowledged for help with obtaining the magnetization curves for our samples.

Supporting Information Available: Procedures for the determination of Co contents by complexiometry and CEMA double bond conversion during photolysis. This material is available free of charge *via* the Internet at http://pubs.acs.org.

REFERENCES AND NOTES

1. Butter, K.; Bomans, P. H. H.; Frederik, P. M.; Vroge, G. J.; Philipse, A. P. Direct Observation of Dipolar Chains in Iron Ferrofluids by Cryogenic Electron Microscopy. *Nat. Mater.* **2003**, *2*, 88–91.
2. Pyun, J. Nanocomposite Materials from Functional Polymers and Magnetic Colloids. *Polym. Rev.* **2007**, *47*, 231–263.
3. de Gennes, P. G.; Pincus, P. A. Pair Correlations in a Ferromagnetic Colloid. *Phys. Kondens. Mater.* **1970**, *11*, 189–198.
4. Tlusty, T.; Safran, S. A. Defect-Induced Phase Separation in Dipolar Fluids. *Science* **2000**, *290*, 1328–1331.
5. Camp, P. J.; Shelley, J. C.; Patey, G. N. Isotropic Fluid Phases of Dipolar Hard Spheres. *Phys. Rev. Lett.* **2000**, *84*, 115–118.
6. Keng, P. Y.; Shim, I.; Korth, B. D.; Douglas, J. F.; Pyun, J. Synthesis and Self-Assembly of Polymer-Coated Ferromagnetic Nanoparticles. *ACS Nano* **2007**, *1*, 279–292.
7. Tripp, S. L.; Dunin-Borkowski, R. E.; Wei, A. Flux Closure in Self-Assembled Cobalt Nanoparticle Rings. *Angew. Chem., Int. Ed.* **2003**, *42*, 5591–5593.
8. Liu, G. J.; Yan, X. H.; Lu, Z. H.; Curda, S. A.; Lal, J. One-Pot Synthesis of Block Copolymer-Coated Cobalt Nanocrystals. *Chem. Mater.* **2005**, *17*, 4985–4991.
9. Safran, S. A. Ferrofluids: Magnetic Strings and Networks. *Nat. Mater.* **2003**, *2*, 71–72.
10. Benkoski, J. J.; Jones, R. L.; Douglas, J. F.; Karim, A. Photocurable Oil/Water Interfaces as a Universal Platform for 2-D Self-Assembly. *Langmuir* **2007**, *23*, 3530–3537.
11. Benkoski, J. J.; Bowles, S. E.; Korth, B. D.; Jones, R. L.; Douglas, J. F.; Karim, A.; Pyun, J. Field-Induced Formation of Mesoscopic Polymer Chains from Functional Ferromagnetic Colloids. *J. Am. Chem. Soc.* **2007**, *129*, 6291–6297.
12. Bowles, S. E.; Wu, W.; Kowalewski, T.; Schalnat, M. C.; Davis, R. J.; Pemberton, J. E.; Shim, I.; Korth, B. D.; Pyun, J. Magnetic Assembly and Pyrolysis of Functional Ferromagnetic Colloids into One-Dimensional Carbon Nanostructures. *J. Am. Chem. Soc.* **2007**, *129*, 8694–8695.
13. Yan, X. H.; Liu, G. J.; Haeussler, M.; Tang, B. Z. Water-Dispersible Polymer/Pd/Ni Hybrid Magnetic Nanofibers. *Chem. Mater.* **2005**, *17*, 6053–6059.
14. Yan, X. H.; Liu, G. J.; Liu, F. T.; Tang, B. Z.; Peng, H.; Pakhomov, A. B.; Wong, C. Y. Superparamagnetic Triblock Copolymer/Fe_2O_3 Hybrid Nanofibers. *Angew. Chem., Int. Ed.* **2001**, *40*, 3593–3596.
15. Li, Z.; Liu, G. J. Water-Dispersible Tetrablock Copolymer Synthesis, Aggregation, Nanotube Preparation, and Impregnation. *Langmuir* **2003**, *19*, 10480–10486.
16. Furst, E. M.; Suzuki, C.; Fermigier, M.; Gast, A. P. Permanently Linked Monodisperse Paramagnetic Chains. *Langmuir* **1998**, *14*, 7334–7336.
17. Cohen-Tannoudji, L.; Bertrand, E.; Bressy, L.; Goubault, C.; Baudry, J.; Klein, J.; Joanny, J. F.; Bibette, J. Polymer Bridging Probed by Magnetic Colloids. *Phys. Rev. Lett.* **2005**, *94*, 14 (038031) .
18. Puntes, V. F.; Krishnan, K. M.; Alivisatos, A. P. Colloidal Nanocrystal Shape and Size Control: The Case of Cobalt. *Science* **2001**, *291*, 2115–2117.
19. Singh, H.; Laibinis, P. E.; Hatton, T. A. Rigid, Superparamagnetic Chains of Permanently Linked Beads Coated with Magnetic Nanoparticles. Synthesis and

Rotational Dynamics under Applied Magnetic Fields. *Langmuir* **2005**, *21*, 11500–11509.
20. Singh, H.; Laibinis, P. E.; Hatton, T. A. Synthesis of Flexible Magnetic Nanowires of Permanently Linked Core-Shell Magnetic Beads Tethered to a Glass Surface Patterned by Microcontact Printing. *Nano Lett.* **2005**, *5*, 2149–2154.
21. Biswal, S. L.; Gast, A. P. Micromixing with Linked Chains of Paramagnetic Particles. *Anal. Chem.* **2004**, *76*, 6448–6455.
22. Doyle, P. S.; Bibette, J.; Bancaud, A.; Viovy, J. L. Self-Assembled Magnetic Matrices for DNA Separation Chips. *Science* **2002**, *295*, 2237.
23. Puntes, V. F.; Zanchet, D.; Erdonmez, C. K.; Alivisatos, A. P. Synthesis of hcp-Co Nanodisks. *J. Am. Chem. Soc.* **2002**, *124*, 12874–12880.
24. Puntes, V. F.; Krishnan, K.; Alivisatos, A. P. Synthesis of Colloidal Cobalt Nanoparticles with Controlled Size and Shapes. *Top. Catal.* **2002**, *19*, 145–148.
25. Murray, C. B.; Sun, S. H.; Gaschler, W.; Betley, T. A.; Kagan, C. R. Colloidal Synthesis of Nanocrystals and Nanocrystal Superlattices. *IBM J. Res. Dev.* **2001**, *45*, 47–55.
26. Sun, S. H.; Murray, C. B. Synthesis of Monodisperse Cobalt Nanocrystals and Their Assembly into Magnetic Superlattices. *J. Appl. Phys.* **1999**, *85*, 4325–4330.
27. Thomas, J. R. Preparation and Magnetic Properties of Colloidal Cobalt Particles. *J. Appl. Phys.* **1966**, *37*, 2914–15.
28. Hess, P. H.; Parker, P. H. Polymers for Stabilization of Colloidal Cobalt Particles. *J. Appl. Polym. Sci.* **1966**, *10*, 1915–1927.
29. Platonova, O. A.; Bronstein, L. M.; Solodovnikov, S. P.; Yanovskaya, I. M.; Obolonkova, E. S.; Valetsky, P. M.; Wenz, E.; Antonietti, M. Cobalt Nanoparticles in Block Copolymer Micelles: Preparation and Properties. *Colloid Polym. Sci.* **1997**, *275*, 426–431.
30. Peng, X. G.; Wickham, J.; Alivisatos, A. P. Kinetics of II−VI and III−V Colloidal Semiconductor Nanocrystal Growth: "Focusing" of Size Distributions. *J. Am. Chem. Soc.* **1998**, *120*, 5343–5344.
31. Zheng, R. H.; Wang, J. D.; Liu, G. J.; Jao, T. C. Lubricant-Oil-Dispersible Stainless-Steel-Binding Block Copolymer Nanoaggregates and Nanospheres. *Macromolecules* **2007**, *40*, 7601–7608.
32. Brandrup, J.; Immergut, E. H. *Polymer Handbook*, 3rd ed.; John Wiley & Sons: New York, 1989; p VII 3−47.
33. Zhulina, E. B.; Borisov, O. V.; Priamitsyn, V. A. Theory of Steric Stabilization of Colloid Dispersions by Grafted Polymers. *J. Colloid Interface Sci.* **1990**, *137*, 495–511.
34. Rosensweig, R. E. *Ferrohydrodynamics*; Cambridge University Press: Cambridge, 1985.
35. Svoboda, J. *Magnetic Techniques for the Treatment of Materials*; Kluwer Academic Publishers: Dordrecht, The Netherlands, 2004.
36. Jeong, U.; Teng, X. W.; Wang, Y.; Yang, H.; Xia, Y. N. Superparamagnetic Colloids: Controlled Synthesis and Niche Applications. *Adv. Mater.* **2007**, *19*, 33–60.
37. Puntes, V. F.; Krishnan, K. M.; Alivisatos, P. Synthesis, Self-Assembly, and Magnetic Behavior of a Two-Dimensional Superlattice of Single-Crystal Epsilon-Co Nanoparticles. *Appl. Phys. Lett.* **2001**, *78*, 2187–2189.
38. Dinega, D. P.; Bawendi, M. G. A Solution-Phase Chemical Approach to a New Crystal Structure of Cobalt. *Angew. Chem., Int. Ed.* **1999**, *38*, 1788–1791.
39. Weast, R. C.; Lide, D. R.; Astle, M. J.; Beyer, W. H. *CRC Handbook of Chemistry and Physics*; 70th ed.; CRC Press: Boca Raton, FL, 1989.
40. Liu, G. J.; Ding, J. F.; Hashimoto, T.; Kimishima, K.; Winnik, F. M.; Nigam, S. Thin Films with Densely, Regularly Packed Nanochannels: Preparation, Characterization, and Applications. *Chem. Mater.* **1999**, *11*, 2233–2240.
41. Guo, A.; Liu, G. J.; Tao, J. Star Polymers and Nanospheres from Crosslinkable Diblock Copolymers. *Macromolecules* **1996**, *29*, 2487–2493.
42. Milner, S. T. Polymer Brushes. *Science* **1991**, *251*, 905–914.
43. Ding, J. F.; Birss, V. I.; Liu, G. J. Formation and Properties of Polystyrene-block-poly(2-cinnamoylethyl methacrylate) Brushes Studied by Surface-Enhanced Raman Scattering and Transmission Electron Microscopy. *Macromolecules* **1997**, *30*, 1442–1448.
44. Tao, J.; Guo, A.; Stewart, S.; Birss, V. I.; Liu, G. J. Polystyrene-block-poly(2-cinnamoylethylmethacrylate) Adsorption in the Buoy-Dominated Regime. *Macromolecules* **1998**, *31*, 172–175.
45. Tao, J.; Guo, A.; Liu, G. J. Adsorption of Polystyrene-block-poly(2-cinnamoylethyl methacrylate) by Silica from Block-Selective Solvent Mixtures. *Macromolecules* **1996**, *29*, 1618–1624.
46. Napper, D. H. *Polymeric Stabilization of Colloidal Dispersions*; Academic Press: London, 1983.
47. Ding, J. F.; Liu, G. J. Polystyrene-block-poly(2-cinnamoylethyl methacrylate) Nanospheres with Crosslinked Shells. *Macromolecules* **1998**, *31*, 6554–6558.
48. Henselwood, F.; Liu, G. J. Water-soluble Porous Nanospheres. *Macromolecules* **1998**, *31*, 4213–4217.
49. Wang, G. C.; Henselwood, F.; Liu, G. J. Water-Soluble Poly(2-cinnamoylethyl methacrylate)-block-Poly(acrylic acid) Nanospheres as Traps for Perylene. *Langmuir* **1998**, *14*, 1554–1559.
50. Liu, G.; Yan, X.; Li, Z.; Zhou, J.; Duncan, S. End Coupling of Block Copolymer Nanotubes to Nanospheres. *J. Am. Chem. Soc.* **2003**, *125*, 14039–14045.
51. Yan, X. H.; Liu, G. J.; Li, Z. Preparation and Phase Segregation of Block Copolymer Nanotube Multiblocks. *J. Am. Chem. Soc.* **2004**, *126*, 10059–10066.
52. Klug, H. P.; Alexander, L. E. *X-Ray Diffraction Procedures for Polycrystalline and Amorphous Materials*; John Wiley & Sons: New York, 1954.